Linear versus nonlinear response of a forced wave turbulence system

Olivier Cadot, Cyril Touzé, Arezki Boudaoud

Linear versus nonlinear response of a forced wave turbulence system

Olivier Cadot and Cyril Touzé
Unité de Recherche en Mécanique (UME), ENSTA-ParisTech, Chemin de la Hunière, 91761 Palaiseau Cedex, France

Arezki Boudaoud
Laboratoire de Physique Statistique, UMR 8550 du CNRS/ENS/Paris 6/Paris 7, 24 rue Lhomond, 75231 Paris Cedex 5, France

A vibrating plate is set into a chaotic state of wave turbulence by a forcing having periodic and random components. Both components are weighted in order to explore continuously intermediate forcing from the periodic to the random one, but keeping constant its rms value. The transverse velocity of the plate is measured at the application point of the force. It is found that whatever the detail of the forcing is, the velocity spectra exhibit a universal cascade for frequencies larger than the forcing frequency range. In contrast, the velocity spectra strongly depend on the nature of the forcing within the range of forcing frequencies. The coherence function is used to extract the contribution of the velocity fluctuations that display a linear relationship with the forcing. The nonlinear contribution to the velocity fluctuations is found to be almost constant, about 55% of the total velocity fluctuations whatever the nature of the forcing from random to periodic. On the other hand, the nonlinear contribution to the fluctuations of the injected power depends on the nature of the forcing; it is significantly larger for the periodic forcing (60%) and decreases continuously as the randomness is increased, reaching a value of 40% for the pure random forcing. For all the cases of intermediate forcing from random to periodic, a simple model of the velocity response recovers in a fairly good agreement the probability density function of the injected power. The consequence of the existence of a linear-response component is discussed in the context of the fluctuation-dissipation theorem validation in experiments of out-of-equilibrium systems.

I. INTRODUCTION

Out-of-equilibrium dissipative systems with a large number of degrees of freedom still display open challenging questions on their statistical distributions of energy and energy fluxes. In the past decade, theoretical advances have emerged by taking into account the chaotic character of the microscopic time evolution [1], leading to important results such as the fluctuation theorem (FT) (or Galavotti-Cohen theorem) [2–4] or the pairing theorem by Dettmann and Morris [5]. However, the extension of these results to turbulent large-scale and dissipative systems is still a matter of debate, and experimental validations do not also provide a clear picture. The first experimental validations of the FT were provided with systems having very few degrees of freedom [6–10] and with forcing being either continuous or periodic but never random. Second, as mentioned in [11,12], the apparent verification of the FT might be hindered by a too small range of explored fluctuation amplitudes or averaging times.

More recent experiments have achieved a correct statistical range, showing that the FT theorem is not fully verified; see, e.g., [13] for the fluctuations of power injection in randomly granular gases, [14] for gravitocapillary waves, [15] for forced turbulence on a free surface, and [16] for a randomly forced plate. Interestingly, all these experimental violations of the FT were found with a forcing having a random component to drive the system out of equilibrium. In the same context, the theoretical results obtained by Farago [17,18] for a Langevin linear model with external random forcing give analytical results for the departure from the FT predictions, so that the experimental results provided in [12] appear as a direct application. More generally, the nature of the forcing [19–21] is often overlooked in the investigation of turbulent systems because it is known to control the injected power statistics. For instance, in [20,21], two different statistics of injected power were achieved by a temporal modification of the forcing, whereas the local turbulent statistical properties were identical in both cases. The discussion above raises the question of the effect of the randomness of the forcing on the dynamics of such a system. We note, however, that this question was recently addressed for a thermal system [22].

In the present paper, a vibrating plate is set into a chaotic state of wave turbulence (WT) by a forcing having both periodic and random components. The vibrating plate provides a perfect setting to study energy fluxes and statistical distributions of global quantities. The WT regime is rather well established [23–25] and the persistence of waves has been experimentally verified [26]. The plate displays a random superimposition of out-of-plane bending waves of broadband frequencies. The first attempt for verifying the FT has been reported in [16], showing a good agreement when the external forcing is periodic, whereas the random forcing leads to an important departure from the theoretical FT prediction. In that context, the natural question arising is that of the influence of the nature of the forcing on the response of the turbulent system and the statistical distribution of global variables.

The paper is organized as follows. Section II provides the details of the experimental setup, allowing a forcing that spans the continuum between the random forcing and the sinusoidal forcing. Section III provides a first decomposition for the velocity field into a turbulent part and a forcing-correlated part, which is tested by predicting the probability density function (PDF) of the injected power. In Sec. IV, this

decomposition is refined using the coherence function in the frequency space, which gives access to the different contributions to the fluctuations of the velocity and the inject power. In Sec. V, the two approaches are compared and the relevance of the results to the FT is discussed.

II. EXPERIMENT AND FORCING

The experimental setup is exactly the same as in [16]. Briefly, a plate is locally forced by a magnet-coil system. The vibrating plate is a steel plate suspended by each of its corners to a rigid frame. The plate was chosen for its very high modal density, obtained by large dimensions, 2 m $\times$ 1 m, for a thickness of $h=0.5$ mm. Material properties were estimated as Young's modulus $E=200$ GPa, Poisson's ratio $\nu=0.3$, and mass per unit volume $\rho=7800$ kg/m^3. The forcing device consists of a coil and a permanent magnet simply magnetized on the steel plate. It has been shown in [27] that in this configuration, the force F acting on the magnet is proportional to the current $I(t)$ circulating in the coil $F(t)=KI(t)$. The current is measured by inserting an Ohmic resistance of 0.12 Ω in series with the coil. The proportionality constant found is $K=0.456$ N/A. The normal velocity v at the application point of the forcing is measured with a laser vibrometer from Polytec (model OFV 056), as in [16]. The normal velocity v and the coil intensity I are simultaneously acquired at the sampling frequency of 5000 Hz. A force signal generated by a PC is amplified with a QSC audio RMX 2450 professional power amplifier which supplies the coil. The force signal is built from a two component function $F'_\alpha(t)$ (where $\alpha\in[0,1]$ represents the proportion of the first (periodic) component and prime symbol x' denotes reduced by standard deviation σ_x) as

$$F'_\alpha(t)=\frac{\alpha}{\beta}S'(t)+\frac{(1-\alpha)}{\beta}\xi'(t). \qquad (1)$$

The first component is a sine function $S'(t)=\sqrt{2}\sin(2\pi f_0 t)$ and the other, a band limited random function $\xi'(t)$. The normalization coefficient $\beta=\sqrt{\alpha^2+(1-\alpha)^2}$ ensures that $\sigma_{F'_\alpha}=1$. The two time series $S'(t)$ and $\xi'(t)$ are generated from a computer using LABVIEW. The sampling rate is 5000 Hz and the time duration 600 s. The frequency of the periodic part is $f_0=75$ Hz. The random part $\xi'(t)$ has been generated by filtering a Gaussian white noise with a bandpass (5–75 Hz) filter. In order to have the current in the coil to be proportional to this force, the voltage signal delivered by the PC has been compensated by the transfer function between the amplifier input and the current circulating in the coil. This transfer function has been measured when applying a white noise as a voltage signal. In Fig. 1, we show the power spectra of the current (proportional to the force applied on the plate) for the two limiting types of forcing, F'_0 for pure random force (with $\alpha=0$) and F'_1 for periodic force (with $\alpha=1$). The random forcing is characterized by a very sharp bandwidth. For intermediate forcing α, this two spectra are combined following Eq. (1). We performed 11 experiments with $\alpha=[0,1]$ by steps of 0.1. The magnitude of the force σ_F has been adjusted to reach a wave turbulence state and remains fairly constant for all the experiments. For each experiment, we measured simultaneously the current circulating in the coil and the velocity of the forcing point with the laser vibrometer. For a given α, time series of a signal represents 2 400 000 points (approximately 600 s long). Auto and cross power spectra are time averaged over windows of 5 s (20 000 points), which gives a frequency resolution of 0.2 Hz. This time averaging is denoted by "$\langle\cdots\rangle$" all the way through the paper.

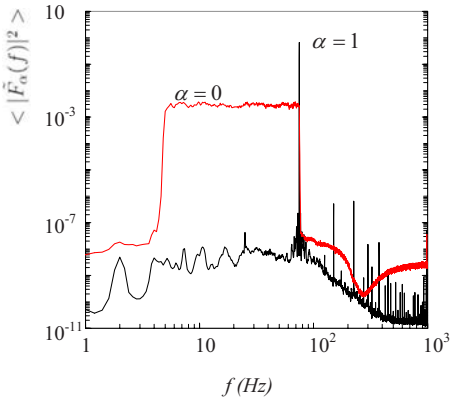

FIG. 1. (Color online) Power spectrum of the force for the two limiting types of forcing: the periodic forcing $\alpha=1$ (black) and the random forcing $\alpha=0$ (red).

III. CORRELATIONS IN THE REAL SPACE

A. Properties of injected power

We consider here the injected power

$$I(t)=v(t)F_\alpha(t). \qquad (2)$$

The mean power $\langle I(t)\rangle$ and its standard deviation σ_I are plotted versus α in Fig. 2. They are normalized using the standard deviations of the force σ_F and of the velocity σ_v. The mean injected (or dissipated) power decreases slightly as the randomness of the force increases. The dependence upon the forcing detail is even more pronounced for the fluctuations

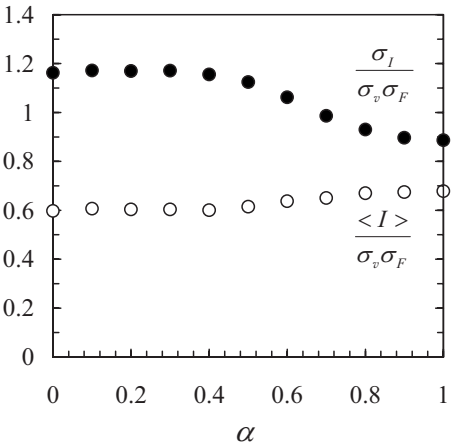

FIG. 2. Normalized mean $\langle I\rangle/\sigma_F\sigma_v$ (or correlation coefficient r) and standard deviation $\sigma_I/\sigma_F\sigma_v$ of the injected power I.

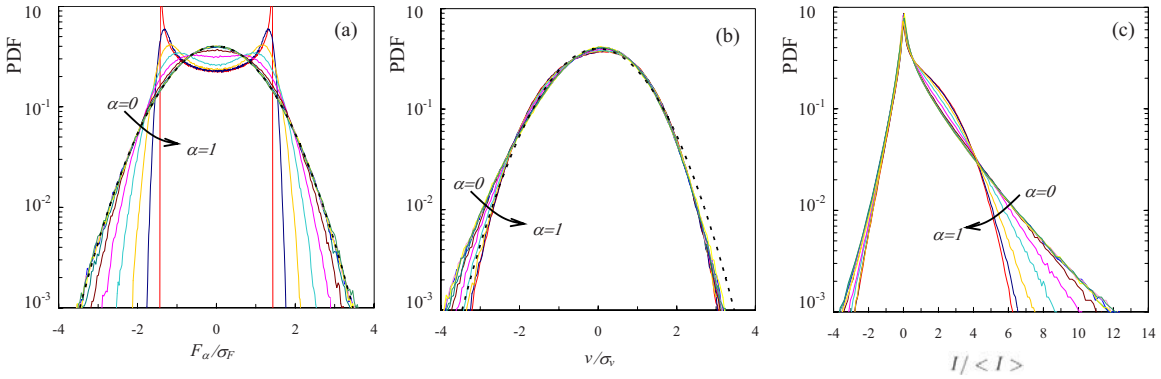

FIG. 3. (Color online) Probability density function of (a) the force, (b) the velocity divided by their standard deviation, and (c) the injected power divided by its mean value versus α spanning [0,1] in steps of 0.1. In (a) and (b), the thick dashed lines are the Gaussian statistics.

σ_I of the injected power. For the pure random forcing the fluctuations are 33% larger than for the pure periodic forcing. Our objective is to understand this strong dependence on the nature of the forcing and its consequences on the measured statistical quantities.

B. Decomposition of the velocity

As the power input is a measurement of the correlation between the velocity v and the force F_α, we first follow [16] and seek a decomposition of the velocity as the sum of two parts—one proportional to the forcing and one uncorrelated with the forcing. We write $v = u + \ell F_\alpha$. The condition that $\langle uF\rangle = 0$ is achieved, say $\langle vF_\alpha\rangle = \ell\langle F_\alpha^2\rangle$, determines the value of ℓ and the velocity decomposition reads

$$v = u + r\frac{\sigma_v}{\sigma_F}F_\alpha, \tag{3}$$

where r is the correlation coefficient between v and F_α, and σ_ϕ stands for the variance of the quantity ϕ. At this stage, Eq. (3) involves the hypothesis that the correlated response is proportional to the force, while any linear operator for ℓ would achieve $\langle uF\rangle = 0$. We will generalize to a linear operator in Sec. IV B.

This decomposition extracts the part of the velocity, the nonlinear feedback u, which does not contribute to the average input power $\langle I\rangle = \langle vF_\alpha\rangle$. The correlation coefficient $r = \langle I\rangle/(\sigma_v\sigma_F)$ is shown in Fig. 2. It has a weak dependence on the forcing detail, with a maximum for the pure periodic forcing ($r = 0.678$) and a minimum for the pure random forcing ($r = 0.589$).

Now we make the hypothesis that u and F_α are statistically independent variables in order to describe the probability density function of the resulting injected power. We further assume that u is Gaussian as it superimposes fluctuations at many scales. In Sec. III C, we investigate whether these hypotheses are consistent with experiments.

C. Probability distributions and predictions for injected power

Using the hypotheses introduced above, we aim at predicting the PDF of the injected power shown.

First, the PDFs of the force and the velocity are displayed in Figs. 3(a) and 3(b). We can check in Fig. 3(a) that as prescribed in Eq. (1), the force statistics change continuously from Gaussian to periodic as α increases from 0 to 1. In contrast, the velocity response statistics in Fig. 3(b) are not very sensitive to the forcing detail. They are rather Gaussian, with a slight negative skewness that increases as the randomness of the forcing increases (as $\alpha \to 0$). The PDFs of the normalized injected power $\frac{I}{\langle I\rangle}$ are plotted in Fig. 3(c). We can observe a significant evolution from exponential tails when the forcing is random ($\alpha = 0$) to Gaussian tails when the forcing is periodic ($\alpha = 1$). These two limiting cases were previously studied in [16]. We can also notice that the PDFs are not sensitive to α when randomness of the forcing is strong as they are all superimposed for α in the range of 0–0.4. We hereafter generalize the work in [16] where two models for the power PDFs were derived for the limiting cases $\alpha = 0$ and $\alpha = 1$. From Eqs. (2) and (3), the injected power reads

$$I = uF_\alpha + r\frac{\sigma_v}{\sigma_F}F_\alpha^2. \tag{4}$$

Then, introducing

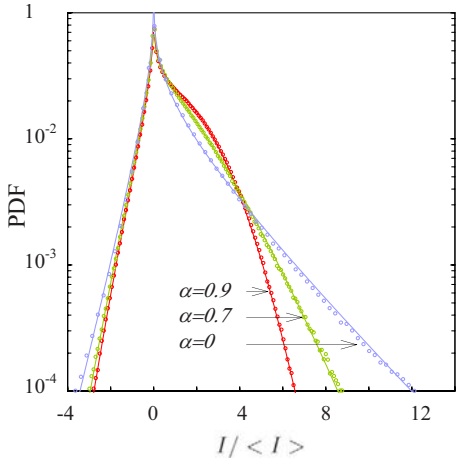

FIG. 4. (Color online) Probability density function of the injected power divided by the mean. Continuous lines are the functions $f_I(\tilde{I})$ in Eq. (12) provided by model (3) for which there is no adjustable parameter.

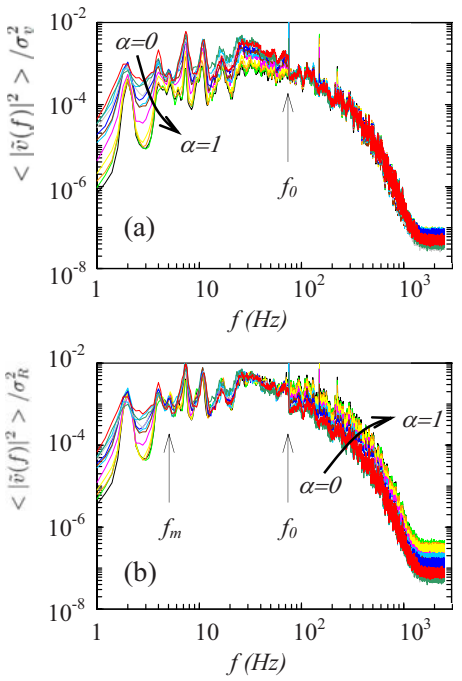

FIG. 5. (Color online) Power spectra of the dimensionless velocity at the application point of the force for α spanning [0,1] in steps of 0.1. In (a), the spectra are presented as $\langle|\tilde{v}(f)|^2\rangle/\sigma_v^2$. In (b), the spectra are presented as $\langle|\tilde{v}(f)|^2\rangle/\sigma_R^2$ (see text). The frequencies f_m=5 Hz and f_0=75 Hz stand for the bounds of the forcing in the frequency space as shown in Fig. 1.

$$q = \frac{r}{\sqrt{1-r^2}}, \tag{5}$$

the PDF of I can be computed as

$$f_I(\tilde{I} = I/\langle I\rangle) = \int f_{F_\alpha}(F'_\alpha) f_u(u') \delta\left(\tilde{I} - \frac{1}{q}F'_\alpha u' - F'^2_\alpha\right) dF'_\alpha du', \tag{6}$$

where f_{F_α}. and f_u are the PDFs of the forcing and of the nonlinear velocity feedback, respectively. We assume this velocity feedback to be Gaussian, as suggested by the nearly Gaussian character of the total velocity [Fig. 3(b)],

$$f_u(u' = u/\sigma_u) = \frac{1}{\sqrt{2\pi}}\exp\left(-\frac{u'^2}{2}\right). \tag{7}$$

From force definition (1), its PDF can be computed as

$$f_{F_\alpha}(F'_\alpha) = \int f_S(S') f_\xi(\xi') \delta\left(F'_\alpha - \frac{\alpha}{\beta}S' - \frac{1-\alpha}{\beta}\xi'\right) dS' d\xi', \tag{8}$$

where

$$f_\xi(\xi') = \frac{1}{\sqrt{2\pi}}\exp\left(-\frac{\xi'^2}{2}\right) \tag{9}$$

is the PDF of the Gaussian noise and

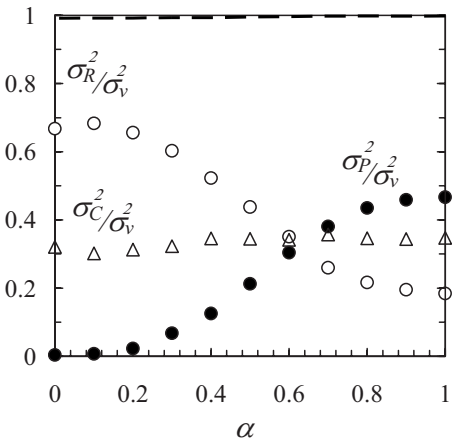

FIG. 6. Contributions of the random frequency domain σ_R^2, periodic frequency domain σ_P^2, and cascade frequency domain σ_C^2 to the energy of the fluctuation defined in Eq. (13) as a function of α; the contributions are normalized by the energy of velocity fluctuations σ_v^2. The dashed line represents the sum of the three terms which is close to 1.

$$f_S(S') = \frac{1}{\pi\sqrt{2-S'^2}} \tag{10}$$

is the PDF of the sinusoidal force. Therefore, Eq. (8) becomes

$$f_{F_\alpha}(F'_\alpha) = \frac{\beta}{(1-\alpha)\sqrt{2\pi^3}}\int_{-\sqrt{2}}^{\sqrt{2}} \frac{1}{\sqrt{2-S'^2}} \times\exp\left[-\frac{1}{2}\left(\frac{\beta F' - \alpha S'}{\alpha - 1}\right)^2\right] dS', \tag{11}$$

while replacing Eq. (7) in Eq. (6) yields the PDF of the injected power as

$$f_I(\tilde{I} = I/\langle I\rangle) = \sqrt{\frac{2}{\pi}}\int_0^\infty \frac{q f_{F_\alpha}(F'_\alpha)}{F'_\alpha} \times\exp\left[-\frac{1}{2}\left(\frac{\beta F'_\alpha - \alpha S'}{\alpha - 1}\right)^2\right] dF'_\alpha. \tag{12}$$

Both integrals (11) and (12) are evaluated numerically.

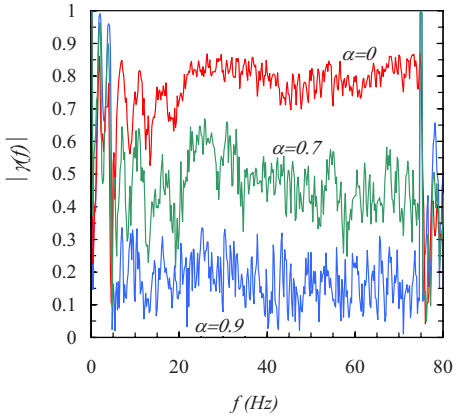

FIG. 7. (Color online) Modulus of the coherence function in the forcing frequency range [5 Hz, 75 Hz] for α=0.9;0.7;0.

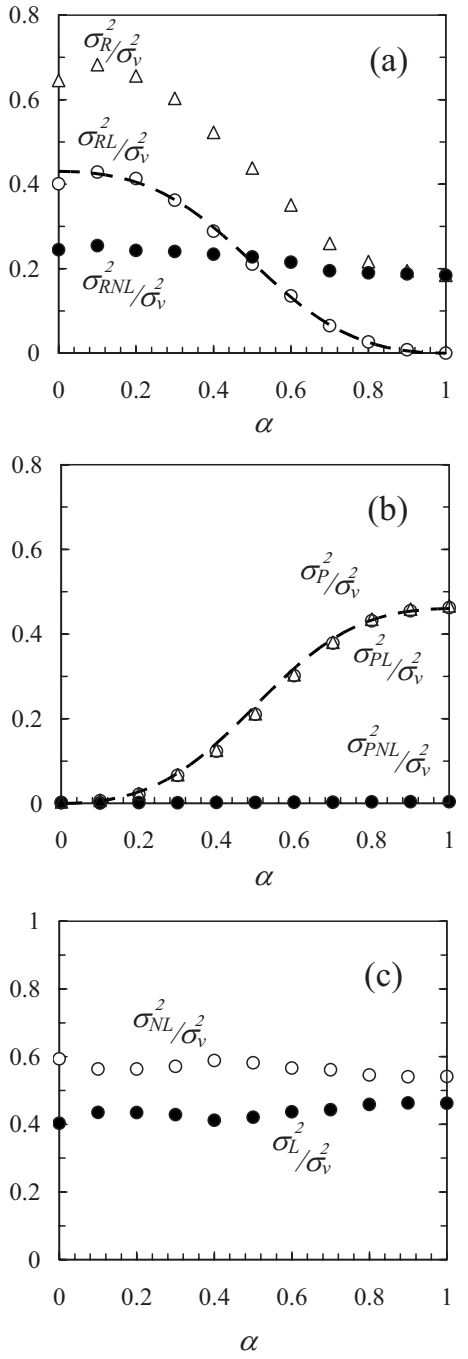

FIG. 8. Decomposition of the velocity fluctuations using the coherence function. (a) Linear (σ_{RL}^2) and nonlinear (σ_{RNL}^2) contributions to energy of the fluctuations in the frequency domain of the random forcing σ_R^2. (b) Linear (σ_{PL}^2) and nonlinear (σ_{PNL}^2) contributions to energy of the fluctuations in the frequency domain of the periodic forcing σ_P^2. Dashed lines are $a_R[(1-\alpha)^2/\beta^2]$ with $a_R=0.43$ in (a) and $a_P(\alpha^2/\beta^2)$ with $a_P=0.46$ in (b), see text. (c) Linear and nonlinear contributions to the energy fluctuation of the velocity response. All contributions are drawn as a function of the forcing nature as defined by α.

It is worth noticing that this model only depends on the correlation coefficient r (measured experimentally) and α (imposed by the forcing). Model (12) is plotted for three different values of $\alpha=0.9;0.7;0$ in Fig. 4. It is found to match the PDF obtained experimentally when varying α in the range [0,1]. It is surprising to find such a good agreement while the PDFs of the velocity are not exactly Gaussian in the experiment as assumed in the model [see Fig. 3(b)]; the injected power is not sensitive to the shape of the PDF of the velocity response but is dominated by the statistics of the imposed force. The case $\alpha=0$ in Eq. (12) is identical to the model used in [14,16].

The success of these predictions shows that it is fair to consider the velocity as a sum of two contributions: one linearly correlated with the forcing and one that is independent from the forcing. However, within this framework, the extraction of either contribution in the time domain would require a better knowledge of the linear response, which is at the moment simply approximated by a proportional model. For instance, a simple phase shift of the linear response in Eq. (3) would lead to different time series of $u(t)$, while the PDF results would remain unchanged. In Sec. IV we aim at identifying these two contributions in the frequency space.

IV. CORRELATIONS IN THE FREQUENCY SPACE

A. Velocity spectrum

The autopower spectra of the velocity $\langle|\tilde{v}(f)|^2\rangle$ are shown in Fig. 5. Notably, for frequencies lower than f_0, the amplitude of the spectra depends on α, while for frequencies larger than f_0, all the spectra are superimposed. It demonstrates that the high-frequency part is insensitive to the nature of the forcing. This observation suggests to decompose the energy of the fluctuations σ_v^2 into three parts, each corresponding to different frequency domains,

$$\sigma_v^2 \approx \sigma_R^2 + \sigma_P^2 + \sigma_C^2. \tag{13}$$

The first energy $\sigma_R^2=\int_{f_m}^{f_0-\delta f_0}\langle|\tilde{v}(f)|^2\rangle df$ corresponds to the frequency domain of the random forcing: $f_m=5$ Hz to $f_0-\delta f_0=74.8$ Hz (excluding the peak at f_0). The second energy corresponds to the narrow domain of the periodic forcing: $\sigma_P^2=\int_{f_0-\delta f_0}^{f_0+\delta f_0}\langle|\tilde{v}(f)|^2\rangle df$ with $\delta f_0=0.2$ Hz. The last energy $\sigma_C^2=\int_{f_0+\delta f_0}^{+\infty}\langle|\tilde{v}(f)|^2\rangle df$ corresponds to the turbulent cascade domain. Looking at Fig. 5(a), we observe that the spectra have similar shapes within the forcing frequency domain, which can be checked by a rescaling using the energy in the random frequency domain, σ_R^2; in Fig. 5(b), all power spectra superimpose satisfactorily within the frequency range [5 Hz, 75 Hz]. The three contributions [Eq. (13)] to the total energy are shown in Fig. 6 for $\alpha\in[0,1]$. The sum is very close to σ_v^2 because contributions for frequencies lower than f_m are negligible. As could be expected from the shape of spectra for $f\rangle 75$ Hz in Fig. 5(a), the contribution of the cascade domain is fairly independent of α.

B. Decomposition of the velocity using the coherence function

Here, we refine the decomposition of Eq. (3). We seek a decomposition of the velocity v in the form of the sum of a turbulent feedback $u(t)$ and a linear response

$$v(t) = u(t) + \mathcal{L}F_\alpha(t). \tag{14}$$

To do so, we define the linear operator $\mathcal{L}$ so that

$$\langle \tilde{u}(f)\tilde{F}_\alpha(f)^*\rangle = 0, \tag{15}$$

where * stands for the complex conjugate and $\tilde{\phi}(f)$ for the Fourier transform of the function ϕ evaluated at the frequency f. We then make the hypothesis that this operator is independent of the forcing. The self-consistent predictions made hereafter will give ground to this hypothesis.

A more direct way to compute $\mathcal{L}$ is to use the coherence function $\gamma(f)$ that measures the correlation between the excitation $F(t)$ and the response $v(t)$ in the frequency space,

$$\gamma(f) = \frac{\langle \tilde{v}\tilde{F}_\alpha^*\rangle}{\sqrt{\langle|\tilde{v}(f)|^2\rangle\langle|\tilde{F}_\alpha(f)|^2\rangle}}. \tag{16}$$

By taking the average of the product of the Fourier transform in Eq. (14) by $\tilde{F}_\alpha^*$ and using $\langle \tilde{u}\tilde{F}_\alpha^*\rangle = 0$, we obtain

$$\gamma(f) = \mathcal{L}_f \sqrt{\frac{\langle|\tilde{F}_\alpha(f)|^2\rangle}{\langle|\tilde{v}(f)|^2\rangle}}, \tag{17}$$

where $\mathcal{L}_f$ is the Fourier representation of the linear operator $\mathcal{L}$ defined as $\mathcal{L}\tilde{F}_\alpha = \mathcal{L}_f\tilde{F}_\alpha$.

The modulus of the coherence, $|\gamma(f)|$, is plotted in Fig. 7 for the frequency domain of the forcing, where the coherence has a meaning. We find that the coherence has a well-defined plateau with a magnitude that increases as α decreases. The pure random forcing is then the most coherent forcing: the linear correlation between the response and the forcing is the strongest. When the periodic forcing is present ($\alpha \neq 0$), the coherence is always 1 at frequency f_0. In the following, we use this coherence function to disentangle the different contributions to the fluctuations of velocity and power input.

C. Coherent and incoherent contributions to the velocity fluctuations

The definition of the operator $\mathcal{L}$ implies that the energy of the fluctuations of the velocity v is the sum of a nonlinear incoherent contribution and linear coherent contributions,

$$\sigma_v^2 = \sigma_u^2 + \langle(\mathcal{L}F_\alpha)^2\rangle. \tag{18}$$

The linear contribution $\sigma_L^2 = \langle(\mathcal{L}F_\alpha)^2\rangle = \langle(\mathcal{L}_f\tilde{F}_\alpha)^2\rangle$ can be computed directly using Eq. (17),

$$\sigma_L^2 = \int_0^\infty |\gamma(f)|^2\langle|\tilde{v}(f)|^2\rangle df. \tag{19}$$

In order to probe the effects of the nature of the forcing, we further decompose the total linear contribution σ_L^2 into two parts, $\sigma_L^2 = \sigma_{RL}^2 + \sigma_{PL}^2$, where

$$\sigma_{RL}^2 = \int_{f_m}^{f_0-\delta f_0} |\gamma(f)|^2\langle|\tilde{v}(f)|^2\rangle df, \tag{20}$$

corresponding to the frequency range of the random forcing, and

$$\sigma_{PL}^2 = \int_{f_0-\delta f_0}^{f_0+\delta f_0} |\gamma(f)|^2\langle|\tilde{v}(f)|^2\rangle df, \tag{21}$$

corresponding to the frequency of the periodic forcing. The nonlinear contributions are deduced by subtraction

$$\sigma_{RNL}^2 = \sigma_R^2 - \sigma_{RL}^2 \tag{22}$$

for the frequency domain of the random forcing and

$$\sigma_{PNL}^2 = \sigma_P^2 - \sigma_{PL}^2 \tag{23}$$

around the frequency of the periodic forcing. The total nonlinear contribution to the fluctuations energy of the velocity response in Eq. (18) is the sum $\sigma_u^2 = \sigma_{NL}^2 = \sigma_{PNL}^2 + \sigma_{RNL}^2$.

Figure 8 shows the results for the different contributions obtained with Eqs. (20)–(23). In the frequency range of the random forcing [see Fig. 8(a)], the fluctuations of the linear response σ_{RL}^2 decrease as α increases and tend to be zero for $\alpha \to 1$ because the coherence function vanishes. The nonlinear response σ_{RNL}^2 has a weaker dependence on the forcing detail, decreasing as α increases. The decrease of σ_{RL}^2 and σ_{RNL}^2 with α could be expected because the random part the force F_α decreases. In the frequency range of the periodic forcing [see Fig. 8(b)], the energy of fluctuations of the nonlinear response is almost zero (the coherence is close to 1 at f_0), while the energy of the linear response increases with α following the weight of the periodic part of the force F_α.

It is worth noticing that the coherence function is exploitable only in the frequency domain of the forcing, say [5 Hz, 75 Hz]. In the other domains, the measured coherence is not strictly equal to zero as it should be in the absence of forcing. This is due to the weak current induced in the coil by the magnet motion according to the vibration of the plate. Hence, the resonant frequencies of the plate are also present in the force signal but at a very low level. This can be seen in Fig. 1 on the spectrum of the periodic force $F_{\alpha=1}$: the background noise below 10^{-7} over the complete frequency range corresponds to the resonances of the plate that are observable on all the velocity spectra in Fig. 5.

D. Predicting the coherent contributions to velocity fluctuations

To push our analysis further, we now compute the linear response σ_L in Eq. (18) using form (1) of the force F_α.

The total energy of the fluctuations of velocity response (18) is written in the Fourier space as

$$\int_0^\infty \langle|\tilde{v}(f)|^2\rangle df = \int_0^\infty \langle|\tilde{u}(f)|^2\rangle + \langle|\widetilde{\mathcal{L}F_\alpha}(f)|^2\rangle df, \tag{24}$$

which using Eq. (1) becomes, for the power spectrum of $v(t)$,

$$\int_0^\infty \langle|\tilde{v}(f)|\rangle^2 df = \int_0^\infty \langle|\tilde{u}(f)|\rangle^2 df + \int_0^\infty \sigma_F^2\frac{\alpha^2}{\beta^2}|\widetilde{\mathcal{L}S'}(f)|^2 df + \int_0^\infty \sigma_F^2\frac{(1-\alpha)^2}{\beta^2}|\widetilde{\mathcal{L}\xi'}(f)|^2 df. \tag{25}$$

Actually, the terms on the right-hand side belong to different

frequency domains. The first term, which accounts for the turbulent feedback, spans all frequencies; the second term vanishes except around the frequency f_0, while the third term is restricted to the bandwidth of the random forcing. Splitting these three terms into the frequency domains of the random forcing, of the periodic forcing, and of the cascade, respectively, we obtain

$$\sigma_R^2 = \int_{f_m}^{f_0-\delta f_0} \langle|\tilde{u}(f)|\rangle^2 df + \sigma_F^2 \frac{(1-\alpha)^2}{\beta^2} \int_{f_m}^{f_0-\delta f_0} |\widetilde{\mathcal{L}\xi'}(f)|^2 df, \tag{26a}$$

$$\sigma_P^2 = \int_{f_0-\delta f_0}^{f_0+\delta f_0} \langle|\tilde{u}(f)|\rangle^2 df + \sigma_F^2 \frac{\alpha^2}{\beta^2} \int_{f_0-\delta f_0}^{f_0+\delta f_0} |\widetilde{\mathcal{L}S'}(f)|^2 df, \tag{26b}$$

$$\sigma_C^2 = \int_{f_0+\delta f_0}^{+\infty} \langle|\tilde{u}(f)|\rangle^2 df. \tag{26c}$$

These three contributions can be rewritten as sums of a linear part and a nonlinear part,

$$\sigma_R^2 = a_R \frac{(1-\alpha)^2}{\beta^2} \sigma_v^2 + \sigma_{RNL}^2, \tag{27a}$$

$$\sigma_P^2 = a_P \frac{\alpha^2}{\beta^2} \sigma_v^2 + \sigma_{PNL}^2, \tag{27b}$$

$$\sigma_C^2 = \sigma_{CNL}^2, \tag{27c}$$

where

$$a_R = \frac{\sigma_F^2}{\sigma_v^2} \int_{f_m}^{f_0-\delta f_0} |\widetilde{\mathcal{L}\xi'}(f)|^2 df \tag{28a}$$

$$\text{and} \quad a_P = \frac{\sigma_F^2}{\sigma_v^2} \int_{f_0-\delta f_0}^{f_0+\delta f_0} |\widetilde{\mathcal{L}S'}(f)|^2 df. \tag{28b}$$

The linear parts of the energy fluctuations, say $\sigma_{RL}^2/\sigma_v^2 = a_R(1-\alpha)^2/\beta^2$ for the random frequency domain and $\sigma_{PL}^2/\sigma_v^2 = a_P\alpha^2/\beta^2$ for the periodic frequency domain, are in good agreement with the measurements displayed in Fig. 8(a). For each case, a_R and a_P are determined by a best fit (see caption of Fig. 8).

This agreement indicates the self-consistency of the decomposition of the velocity into a linear part and a nonlinear part [Eq. (14)]. We thus obtain a reliable measurement of the corresponding contributions to the energy of velocity fluctuations, $\sigma_v^2 = \sigma_{NL}^2 + \sigma_L^2$, as a function of the detail of the forcing α, where

$$\sigma_{NL}^2 = \sigma_{RNL}^2 + \sigma_{PNL}^2 + \sigma_C^2, \quad \sigma_L^2 = \sigma_v^2 - \sigma_{NL}^2. \tag{29}$$

Both contributions are plotted in Fig. 8(c). It can be seen that the forcing detail α does not affect much the relative weight of these contributions. The nonlinear response is always found to be slightly larger than the linear response, about 55% of the total-energy fluctuations.

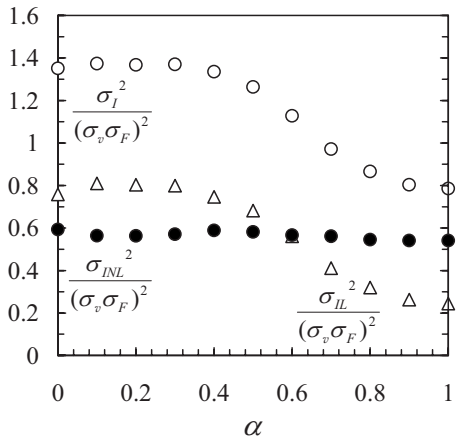

FIG. 9. Linear σ_{IL} and nonlinear σ_{INL} contributions to the injected power fluctuations σ_I, normalized using the standard deviations of the velocity σ_v and force σ_F.

E. Coherent and incoherent contributions to the fluctuations of the injected power

We now turn to the fluctuations of the injected power,

$$I(t) = v(t)F(t). \tag{30}$$

Similarly to the velocity, we can extract from the energy of the injected power fluctuation the contributions due to linear and nonlinear responses.

Using decomposition (14) of the velocity response, the injected power is rewritten as

$$I = uF_\alpha + \mathcal{L}F_\alpha F_\alpha, \tag{31}$$

which leads to both nonlinear and linear contributions,

$$\sigma_I^2 = \sigma_u^2 \sigma_{F_\alpha}^2 + \langle (\mathcal{L}F_\alpha F_\alpha - \langle \mathcal{L}F_\alpha F_\alpha \rangle)^2 \rangle. \tag{32}$$

The nonlinear contribution which is the first right-hand side term in Eq. (32) is calculated directly from the nonlinear contribution of the velocity response, $\sigma_{INL}^2 = \sigma_u^2 \sigma_{F_\alpha}^2 = \sigma_{NL}^2 \sigma_{F_\alpha}^2$, while the linear contributions is simply deduced from $\sigma_{IL}^2 = \sigma_I^2 - \sigma_{INL}^2$. Figure 9 shows both linear and nonlinear contributions to the total fluctuation energy of the injected power. The nonlinear contribution σ_{INL}^2 remains fairly constant whatever the forcing detail α is. In contrast, the linear one, σ_{IL}^2, is very sensitive to the forcing detail and increases with the randomness of the forcing. Hence, for the pure periodic forcing ($\alpha = 1$), the dominant response in the power fluctuations is nonlinear, while for the random forcing ($\alpha = 0$) the dominant response is linear.

V. DISCUSSION

A. Relation between the two decompositions of the velocity

In the decomposition of the velocity following Eq. (14), the Fourier representation of the linear operator $\mathcal{L}$ could be computed using the coherence function. The first decomposition [Eq. (3)] amounts to stating that

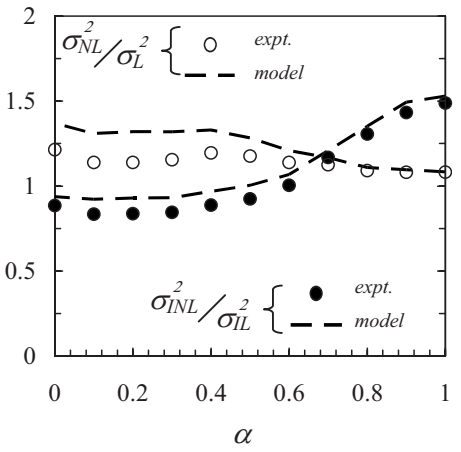

FIG. 10. Ratio of the nonlinear to linear response for the velocity and the injected power. Proportional model (3) for the linear response (dashed lines) is compared to the experimental data using the coherence decomposition (symbols).

$$\mathcal{L} = r\frac{\sigma_v}{\sigma_F} \tag{33}$$

is a constant (r is the correlation coefficient between the force F and the velocity), which is the simplest approximation possible. We will refer to this decomposition as the proportional model.

Using Eq. (33), we can compute the linear response in Eq. (26a) for the random frequency domain and in Eq. (26b) for the periodic frequency domain. The proportional model yields $a_P = a_R = r^2$. The correlation coefficient $r = \langle I \rangle / (\sigma_F \sigma_v)$ was shown in Fig. 2. For the pure periodic forcing, the measured value of r gives $a_P = r^2 = 0.46$, which matches exactly the value given by the best fit in Fig. 8(c). When randomness is introduced, the best fit gives $a_R = 0.43$ which is different from r^2 as predicted just above. Nevertheless, a_R remains close to r^2. All this means that the Fourier representation of the linear operator is actually close to a constant.

B. Linear response vs nonlinear response

The fluctuations of the response of the plate have been decomposed into a linear (coherent) component and a nonlinear (incoherent turbulent feedback) component.

(a) For the velocity response, the ratio between these two contributions is fairly constant; the nonlinear contribution, σ_{NL}, is always slightly larger than the linear one, σ_L (see white symbols in Fig. 10). The proportional model gives a good estimation of this ratio, especially on the side of the periodic forcing (close to $\alpha = 1$).

(b) Concerning the injected power fluctuations, the ratio of nonlinear to linear fluctuations varies significantly with the forcing detail. The energy of fluctuations due to the turbulent feedback, σ_{INL}, is clearly dominant for a periodic forcing while it is smaller than the linear part of fluctuations, σ_{IL}, for a random forcing. Actually we can even observe in Fig. 9 that the variations of the total power fluctuation are completely ascribed to the linear part of the fluctuations.

This discrepancy between the velocity and energy input could appear for other global quantities characterizing a turbulent system because global quantities often reside in the frequency domain of the forcing and then mix linear and nonlinear responses. While the nonlinear response could be universal, the linear one is certainly not. For instance, a global quantity such as the injected energy on long times has been extensively studied in the framework of the Gallavotti-Cohen theorem (or fluctuation-dissipation theorem). One might wonder about the range of applicability of this theorem. An answer is given by the theoretical work of Farago [17,18] on the linear case of a particle submitted to viscous damping and a random Gaussian external force. He found that the conclusions of the theorem are not met. Experimentally, when a wave turbulence system is randomly forced Falcon *et al.* [14] and Cadot *et al.* [16] showed that results are very similar to those of Farago [17,18]. In [16], the same system was forced periodically, and the conclusions of the theorem were met. The present work gives the explanation that the random forcing is dominated by the linear response that might invalidate the application of the theorem. One could therefore speculate that the FT only concerns the nonlinear part of the power fluctuations.

VI. CONCLUSION

The wave turbulence state of a vibrating plate was studied when the driving spans the continuum between a periodic force and a random force, but keeping the same rms fluctuations. Using the coherence function, we were able to disentangle the linear contribution to the velocity fluctuations from the nonlinear ones. Furthermore, a simple additive model consisting of a linear proportional part and a turbulent feedback allowed us to recover the statistics of the injected power.

The main experimental finding is that, when the forcing is random, the linear response dominates the energy of the fluctuations of the injected power, while in contrast, the nonlinear response dominates for the periodic forcing. This result may help understanding the observation [13–16] of the invalidation of the fluctuation theorem [2–4] for randomly forced systems, while it seems to be applicable to deterministically forced ones [16].

[1] D. Ruelle, J. Stat. Phys. **95**, 393 (1999).

[2] D. J. Evans, E. G. D. Cohen, and G. P. Morriss, Phys. Rev. Lett. **71**, 2401 (1993).

[3] G. Gallavotti and E. G. D. Cohen, Phys. Rev. Lett. **74**, 2694 (1995).

[4] D. J. Evans and D. J. Searles, Phys. Rev. E **50**, 1645 (1994).

[5] C. P. Dettmann and G. P. Morriss, Phys. Rev. E **53**, R5545 (1996).

[6] G. M. Wang, E. M. Sevick, E. Mittag, D. J. Searles, and D. J. Evans, Phys. Rev. Lett. **89**, 050601 (2002).

[7] S. Schuler, T. Speck, C. Tietz, J. Wrachtrup, and U. Seifert, Phys. Rev. Lett. **94**, 180602 (2005).
[8] N. Garnier and S. Ciliberto, Phys. Rev. E **71**, 060101 (2005).
[9] F. Douarche, S. Joubaud, N. B. Garnier, A. Petrosyan, and S. Ciliberto, Phys. Rev. Lett. **97**, 140603 (2006).
[10] P. Jop, A. Petrosyan, and S. Ciliberto, EPL **81**, 50005 (2008).
[11] S. Aumaître, S. Fauve, S. McNamara, and P. Poggi, Eur. Phys. J. B **19**, 449 (2001).
[12] C. Falcón and E. Falcon, Phys. Rev. E **79**, 041110 (2009).
[13] P. Visco, A. Puglisi, A. Barrat, E. Trizac, and F. van Wijland, J. Stat. Phys. **125**, 529 (2006).
[14] E. Falcon, S. Aumaître, C. Falcón, C. Laroche, and S. Fauve, Phys. Rev. Lett. **100**, 064503 (2008).
[15] M. M. Bandi and C. Connaughton, Phys. Rev. E **77**, 036318 (2008).
[16] O. Cadot, A. Boudaoud, and C. Touzé, Eur. Phys. J. B **66**, 399 (2008).
[17] J. Farago, J. Stat. Phys. **107**, 781 (2002).
[18] J. Farago, Physica A **331**, 69 (2004).
[19] O. Cadot, Y. Couder, A. Daerr, S. Douady, and A. Tsinober, Phys. Rev. E **56**, 427 (1997).
[20] J. H. Titon and O. Cadot, Phys. Fluids **15**, 625 (2003).
[21] O. Cadot and J. H. Titon, Phys. Fluids **16**, 2140 (2004).
[22] J. Gomez-Solano, L. Bellon, A. Petrosyan, and S. Ciliberto, EPL **89**, 60003 (2010).
[23] G. Düring, C. Josserand, and S. Rica, Phys. Rev. Lett. **97**, 025503 (2006).
[24] A. Boudaoud, O. Cadot, B. Odille, and C. Touzé, Phys. Rev. Lett. **100**, 234504 (2008).
[25] N. Mordant, Phys. Rev. Lett. **100**, 234505 (2008).
[26] P. Cobelli, P. Petitjeans, A. Maurel, V. Pagneux, and N. Mordant, Phys. Rev. Lett. **103**, 204301 (2009).
[27] O. Thomas, C. Touzé, and A. Chaigne, J. Sound Vib. **265**, 1075 (2003).